15.2 EVOLUTION OF A TORNADIC SUPERCELL AND ITS ENVIRONMENT SAMPLED BY THE NWRT PHASED ARRAY RADAR AND OKLAHOMA CITY MICRONET

Rick M. Hluchan *
University of Oklahoma/National Severe Storms Laboratory, Norman, Oklahoma

Pamela L. Heinselman, NOAA/National Severe Storms Laboratory, Norman, Oklahoma

Rodger A. Brown, NOAA/National Severe Storms Laboratory, Norman, Oklahoma

1. INTRODUCTION

Previous studies have investigated cyclic supercells and how these storms can periodically undergo several life cycles during their lifetime (e.g., Darkow and Roos 1970; Burgess et al. 1982; Wakimoto et al. 2003; Beck et al. 2006; French et al. 2008). Some cyclic supercells produce a number of tornadoes over their lifetime; a process known as cyclic tornadogenesis (e.g., Burgess et al. 1982; Dowell and Bluestein 2002). Every cyclic supercell, however, does not produce a tornado each time the supercell cycles (French et al. 2008).

Various studies have also examined the merging of supercell storms (e.g., Lemon 1976; Kogan and Shapiro 1996) and multicell storms (Westcott 1984; Westcott 1994), but few have documented the interactions of small convective cells merging with supercells (Finley et al. 2001; Lee et al. 2006; Wurman et al. 2007). Little is known about what influence convective cells have when merging with a supercell during its cyclic process. The current knowledge of merging, in the majority of the above studies, is based on the use of mechanically steered Doppler radars that have update times more than 4 min or are focused on low elevation angles only.

* *Corresponding author address:* Rick M. Hluchan, National Severe Storms Laboratory, 120 David L. Boren Blvd., Suite 4340, Norman, Oklahoma, 73072. E-mail: rick.hluchan@noaa.gov

On 10 February 2009, a cyclic supercell produced two tornadoes as it moved across the western side of Oklahoma City (Fig. 1). As the storm cycled, numerous updrafts developed and moved through the supercell at various locations. During its lifetime the storm was sampled approximately every minute by the National Weather Radar Testbed Phased Array Radar (NWRT PAR). Surface state variables were measured as the supercell also moved across several surface stations of the Oklahoma City Micronet (Basara et al. 2009) and Oklahoma Mesonet (Brock et al. 1995; McPherson et al. 2007).

Rapid updates revealed multiple divergence signatures within the supercell indicative of individual updrafts. These transitory updrafts lasted up to 25 min and tended to form southeast of the main updraft and south of the mesocyclones. This study examines the propensity and evolutionary characteristics of these updrafts and their temporal and spatial relation to cyclic mesocylogenesis and tornadogenesis.

Section 2 of this study describes this unique dataset further. The synoptic conditions preceding the event are discussed in section 3. Results of the radar analysis, found within section 4, provides observational insight regarding main and transient updrafts within the supercell. Concluding remarks are found in section 5.

Table 1. PAR radar and scanning strategy characteristics for 10 February 2009.

PAR Operating Characteristics	
Wavelength	9.38 cm
Transmitted peak power	750 kW
Range resolution	240 m
Half–power beamwidth	1.50°–2.10°
Azimuthal sample interval	1.0°
Nyquist velocity	23.8 m s^{-1}
Elevation angles	0.51°–15.50°; 0.51°–38.80° 14 elevations
Data interval	32–70 s
Range to tornado	38–55 km
0.51° beam height	0.8–1 km

2. PHASED ARRAY RADAR

Important operating characteristics of the NWRT PAR are given in Table 1; more details about the PAR are found in Zrnić et al. (2007). One significant advantage of the PAR is its antenna design. The antenna forms and steers the beam in azimuth and elevation electronically which allows the operator to focus on weather echo without moving the radar. The PAR is currently equipped with a single-faced phased array that scans sectors up to 90° in azimuth. Stationary scanning provides high–temporal resolution data while sampling the atmosphere without beam smearing.

The Oklahoma City 10 February 2009 tornadic supercell passed within 37 km of the PAR (Fig. 1), which scanned almost continuously throughout the evolution of the storm. During this event the radar was operated using two scanning strategies (Table 1). At the beginning of data collection (2023–2044 UTC), when the supercell was 37–41 km from the PAR, data were collected at 14 elevation angles between 0.51° and 15.50°. As the supercell moved beyond 41 km of the PAR (2044–2117 UTC) data were collected between the angles of 0.51° and 38.80°. Both scanning strategies completed a full volume scan in approximately 70 s; with the lowest tilt being revisited halfway through the scan to improve temporal resolution at that level. Lowest elevation angle (0.51°) beam heights relative to the circulation were 0.8 km AGL at the beginning of data collection and 1 km AGL at the end of the period of interest.

3. SYNOPTIC ENVIRONMENT

During the early afternoon hours on 10 February 2009, a strong surface low pressure system was positioned over Minnesota with a baroclinic zone draped across southern Oklahoma. A series of shortwave troughs at 700 mb aided lift over central Oklahoma. A developing jet streak at 300 hPa supported an area of upper–level divergence over much of the Southern Plains (e.g., Uccellini and Johnson 1979). An intense upper low and associated long wave trough were approaching from the southwest US, acting to increase both speed and directional wind shear for supercell development.

A north–south oriented dryline extended across western Oklahoma where a sharp moisture gradient existed (Fig. 2). An examination of the 1800 UTC Norman sounding showed a significant increase in moisture since 1200 UTC throughout the mid– and low–levels of the atmosphere (Fig. 3). Surface dewpoints across central

Oklahoma increased nearly 15°C between 1200 UTC and 1800 UTC due to winds at the surface increasing and backing to the southeast in response to a developing low over southeastern Colorado. As a result of the increase in tropospheric moisture convective available potential energy (CAPE) values near 500 J kg^{-1} were present within the area of strong insolation where storms formed.

4. RESULTS

4.1 Overview

The PAR sampled several severe thunderstorms as they formed across central Oklahoma along a moisture gradient. The 10 February 2009 cyclic supercell was sampled from 2023–2105 UTC as it passed within 37–55 km of the radar site. At 2023 UTC this supercell contained a mesocyclone in its mature stage (Fig. 4) (Burgess et al. 1982), which extended to 3.1 km AGL. As the mesocyclone began to dissipate (2028 UTC) and the supercell (2034 UTC) produced a short–lived (~1 min), weak EF1 tornado, another mesocyclone formed east of the old circulation and initiated a new cycle of the supercell. The supercell, containing the new mesocyclone, then produced (2052 UTC) an EF2 tornado, lasting approximately 12 min toward the end of its lifetime (Fig. 1).

The supercell also contained two primary updrafts. As one updraft began to dissipate at 2049 UTC, another updraft formed 2 km to its west and was maintained through the end of the analysis period (2105 UTC). These updrafts extended from the lowest elevation scan to 12.4 km AGL. Each updraft was identified as having convergence near the surface transitioning to divergence aloft in the PAR storm–relative velocity field as air inside the updrafts increasingly spread radially outward with height (Fig. 4a) (Byers and Braham 1948). To quantify this divergence, the circular mesocyclone model developed by Desrochers and Harris (1996) was used. In their model, horizontal divergence is assumed uniform in the central, core region and is given by

$$D = \frac{2V_{rad}}{R} \quad (1)$$

where R is distance between velocity peaks. From single–Doppler data, the parameter V_{rad} can be evaluated as the outgoing velocity peak minus the incoming velocity peak divided by 2. (1) Assumes pure divergence since the zero line separating the velocity peaks is oriented perpendicular to the radar beam.

The initial main updraft (referred to as main UD 1) was associated with divergence extending from 5 to 9 km AGL at the starting time of analysis (2023 UTC) (Fig. 5). This divergence was located close to a strong reflectivity gradient at the western–most edge of the supercell (Fig. 4a). Beginning around 2026 UTC, this divergence began to strengthen above 10 km AGL and peaked at 2032 UTC with an estimated value of 0.03 s^{-1} at ~12.5 km indicating a strengthening updraft. Two minutes later (2034 UTC) the supercell produced its first tornado. Divergence then quickly dissipated above 10 km AGL but remained below this level down to 6 km AGL (Fig. 5). The depth of divergence began to decrease again by 2043 UTC, and the divergence signature associated with main UD 1 completely dissolved by 2049 UTC indicating updraft demise.

Beginning at 2044 UTC continuing to the end of the analysis period, less dense vertical sampling produced less detailed observations of divergence. Shortly after adopting a new scanning strategy (2049 UTC), another divergence signature (referred to as main UD 2) developed near the area where main UD 1 had dissipated. Main UD 2 persisted until 2104 UTC and the associated divergence extended from around 6 km AGL to 11.5 km AGL throughout its duration (Fig. 6). Divergence remained relatively weak until 2101 UTC

when it peaked at 0.023 s^{-1} near 11.5 km AGL. After this peak, divergence was limited to between 9 and 10 km AGL.

4.2 Transient Updrafts

As the 10 February 2009 supercell moved across central Oklahoma, several secondary updrafts developed on the southern flank of the supercell. In all, 6 of these updrafts, not including the 2 primary updrafts, were examined. The updrafts shared several characteristics in common. Each individual updraft tended to develop southeast of the main updraft on the southwest edge a strong reflectivity gradient and move northeast, through the supercell. Divergence associated with each updraft developed near 5 km AGL and extended to ~12 km AGL and lasted approximately 15–20 min. The intensity of each updraft's divergence varied with time and height.

A representative updraft (referred to as UD C) developed about 5 km southeast of main UD 1 at 2035 UTC (Fig. 7a). Divergence associated with this updraft initiated at 5 km AGL and 14 min later (2049 UTC) extended to a maximum height of 11.1 km AGL (Fig. 8). Divergence values in the PAR storm–relative velocity field were initially strong (0.031 s^{-1}) near 6.1 km AGL at 2037 UTC and remained relatively steady throughout the updraft's lifetime (Fig. 7b). After 2045 UTC until the end of UD C's lifetime, there was a significant increase in height of the divergence signature (Fig. 8). As time progressed, UD C moved northeast and divergence eventually weakened with height beginning around 5.5 km AGL (Fig. 7c and 8). Divergence associated with UD C completely dissipated by 2052 UTC.

Perhaps most important is the updraft's location relative to other features associated with the supercell. One particular updraft (Fig. 4) (referred to as UD B) appeared to be associated with a convective cell that merged with the supercell near its southern flank just before the analysis period (not shown). At the start of analysis (2023 UTC), UD B was located about 7 km southeast of the primary updraft and about 3 km southwest of the initial mesocyclone moving northeast (Figs. 4a and b). UD B's divergence signature at this time was weak (0.014 s^{-1}) and only discernable at 4.9 km AGL. By 2033 UTC, UD B's divergence signature reached its maximum intensity with a value of 0.043 s^{-1} at 8.2 km AGL (Fig. 9). At the same time at 2.4°, the first mesocyclone weakened aloft (Figs. 4b and 10b), but the low–level circulation contracted and strengthened rapidly (Fig. 10c). Perhaps coincidentally, the divergence signature associated with UD B became nearly vertically aligned with the mesocyclone and low–level circulation (Fig. 10). Approximately 1 min later the supercell produced its first tornado. The EF1 tornado, lasting ~1 min, tracked 1.2 km through northwest Oklahoma City producing minor damage (Fig. 1).

UD B reached its maximum height of 11.8 km AGL at 2037 UTC and was now located about 6 km southeast of the main updraft (Fig. 11a). As the supercell's first mesocyclone and tornado turned northeast, away from UD B, they quickly dissipated by 2037 UTC. A new mesocyclone had developed at the same time and was deepening about 2 km east of the previous mesocyclone (Fig. 11b). This mesocyclone developed aloft at 2 km AGL near a bulge in the northeast segment of the rear flank gust front suggesting tilting of horizontal vorticity in the gust front (Figs. 11c and 12). UD B had continued to move northeast and at 2037 UTC became vertically aligned with the new mesocyclone (Fig. 11). By 2040 UTC, UD B had moved away from the new mesocyclone and began to weaken (Fig. 9). UD B was similar to the primary updrafts with respect to divergence longevity and depth (Fig. 9).

5. Summary

The 10 February 2009 Oklahoma City cyclic, tornadic supercell represents a unique case in which high–temporal and spatial resolution data were collected by the

PAR and the Oklahoma City Micronet. The combination of increased temporal and spatial resolution revealed numerous updrafts within the supercell.

The supercell contained two main updrafts and six transient updrafts during the analysis period. The main updrafts remained located on the strong reflectivity gradient at the southwest edge of the supercell. Each updraft was associated with divergence signatures aloft in the PAR storm relative velocity.

The transient updrafts shared very similar evolutionary characteristics. Divergence associated with each updraft developed initially near 5 km AGL and extended as high as 12 km AGL. Each updraft lasted 15–20 min and moved northeast while initially developing on the southwest edge of a strong reflectivity gradient, but then moving through the supercell (Fig. 7).

One of these transitory updrafts (UD B), developed similar to the other updrafts and became nearly vertically aligned with a low–level circulation just prior to the supercell producing its first tornado (2034 UTC). Though few minutes later (2037 UTC), UD B reached its maximum height and became vertically aligned with the new mesocyclone, its associated divergence signature dissipated 3 min later.

Future analysis will investigate how the other transient updrafts evolved with respect to the second tornado.

Acknowledgements. The authors would like to thank Dave Andra and Patrick Burke of the Norman WFO for providing insight on the synoptic conditions. We further recognize: Jeff Basara of the Oklahoma Climate Survey for helping provide the Oklahoma City Micronet data and Adam Smith and Kevin Manross (CIMMS/NSSL) for their technical contributions to display the data.

REFERENCES

Basara, J. B., B. G. Illston, C. A. Fiebrich, R. A. McPherson, J. P. Bostic, P. Browder, D. B. Demko, C. Morgan, and K. Kesler, 2009: An overview of the Oklahoma City Micronet. Preprints, *8th Symposium on the Urban Environment*, Phoenix, AZ, Amer. Meteor. Soc., J1.1.

Beck, J. R., J. L. Schroeder, J. M. Wurman, 2006: High-resolution dual-doppler analyses of the 29 May 2001 Kress, Texas, cyclic supercell. *Mon. Wea. Rev.*, **134**, 3125–3148.

Brock, F. V., K. C. Crawford, R. L. Elliott, G. W. Cuperus, S. J. Stadler, H. L. Johnson, and M. D. Eilts, 1995: The Oklahoma Mesonet: A technical overview. *J. Atmos. Oceanic Technol.,* **12**, 5–19.

Burgess, D. W., V. T. Wood, and R. A. Brown, 1982: Mesocyclone evolution statistics. Preprints, *12th Conf. on Severe Local Storms,* San Antonio, TX, Amer. Meteor. Soc., 422–424.

Byers, H. R., and R. R. Braham, 1948: Thunderstorm structure and circulation. *J. Meteor.,* **5**, 71–86.

Darkow, G. L., and J. C. Roos, 1970: Multiple tornado producing thunderstorms and their apparent cyclic variations in intensity. Preprints, 14th Conf. on Radar Meteorology, Tucson, AZ, Amer. Meteor. Soc., 305–308.

Desrochers, P. R., and F. I. Harris, 1996: Interpretation of mesocyclone vorticity and divergence structure from single–Doppler radar. *J. Appl. Meteor.,* **35**, 2191–2209.

Dowell, D. C., and H. B. Bluestein, 2002: The 8 June 1995 McLean, Texas, storm. Part I: Observation of cyclic tornadogenesis. *Mon. Wea. Rev.,* **130**, 2626–2648.

Finley, C. A., W. R. Cotton, and R. A. Pielke, 2001: Numerical simulation of tornadogenesis in a high-precipitation supercell. Part I: Storm evolution and transition into a bow echo. J. Atmos. Sci., **58**, 1597–1629.

French, M. M., H. B. Bluestein, D. C. Dowell, L. J. Wicker, M. R. Kramar, and A. L. Pazmany, 2008: High-resolution, mobile Doppler radar observations of cyclic

mesocyclogenesis in a supercell. *Mon. Wea. Rev.*, **136**, 4997–5016.

Kogan, Y. L., and A. Shapiro, 1996: The Simulation of a convective cloud in a 3D model with explicit microphysics. Part II: Dynamical and microphysical aspects of cloud merger. J. Atmos. Sci., **53**, 2525–2545.

Lee, B. D., B. F. Jewett, and R. B. Wilhelmson, 2006: The 19 April 1996 Illinois tornado outbreak. Part II: Cell mergers and associated tornado incidence. Wea. Forecasting, **21**, 449–464.

Lemon, L. R., 1976: The flanking line, a severe thunderstorm intensification source. J. Atmos. Sci., **33**, 686–694.

McPherson, R. A., C. Fiebrich, K. C. Crawford, R. L. Elliott, J. R. Kilby, D. L. Grimsley, J. E. Martinez, J. B. Basara, B. G. Illston, D. A. Morris, K.A. Kloesel, S. J. Stadler, A. D. Melvin, A. J. Sutherland, and H. Shrivastava, 2007: Statewide monitoring of the mesoscale environment: A technical update on the Oklahoma Mesonet. *J. of Atmos. Oceanic Technol.,* **24**, 301–321.

Uccellini, L. W., and D. R. Johnson, 1979: The coupling of upper and lower tropospheric jet streaks and implications for the development of severe convective storms. *Mon. Wea. Rev.*, **107**, 682–703.

Wakimoto, R. M., H. V. Murphey, D. C. Dowell, H. B. Bluestein, 2003: The Kellerville tornado during VORTEX: Damage survey and Doppler radar analyses. *Mon. Wea. Rev.*, **131**, 2197–2221.

Westcott, N., 1984: A historical perspective on cloud mergers. Bull. Amer. Meteor. Soc., **65**, 219–226.

———, 1994: Merging of convective clouds: Cloud initiation, bridging, and subsequent growth. Mon. Wea. Rev., **122**, 780–790.

Wurman, J., Y. Richardson, C. Alexander, S. Weygandt, and P. F. Zhang, 2007: Dual-Doppler and single-Doppler analysis of a tornadic storm undergoing mergers and repeated tornadogenesis. Mon. Wea. Rev., **135**, 736–758.

Zrnic, D. S., J. F. Kimpel, D. E. Forsyth, A. Shapiro, G. Crain, R. Ferek, J. Heimmer, W. Benner, T. J. McNellis, and R. J. Vogt, 2007: Agile–beam phased array radar for weather observations. *Bull. Amer. Meteor. Soc*., **88**. 1753–1766.

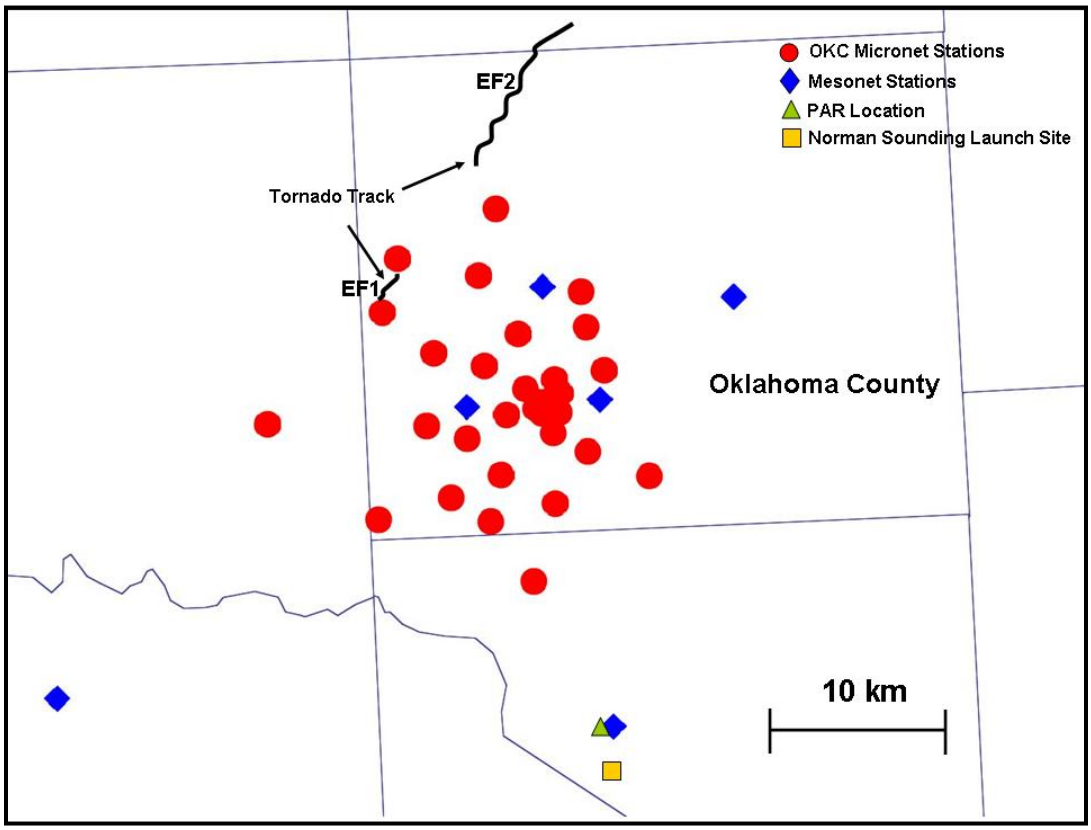

Fig. 1. Tornado tracks and locations of Oklahoma City Micronet and Mesonet stations, PAR, and the Norman sounding launch site.

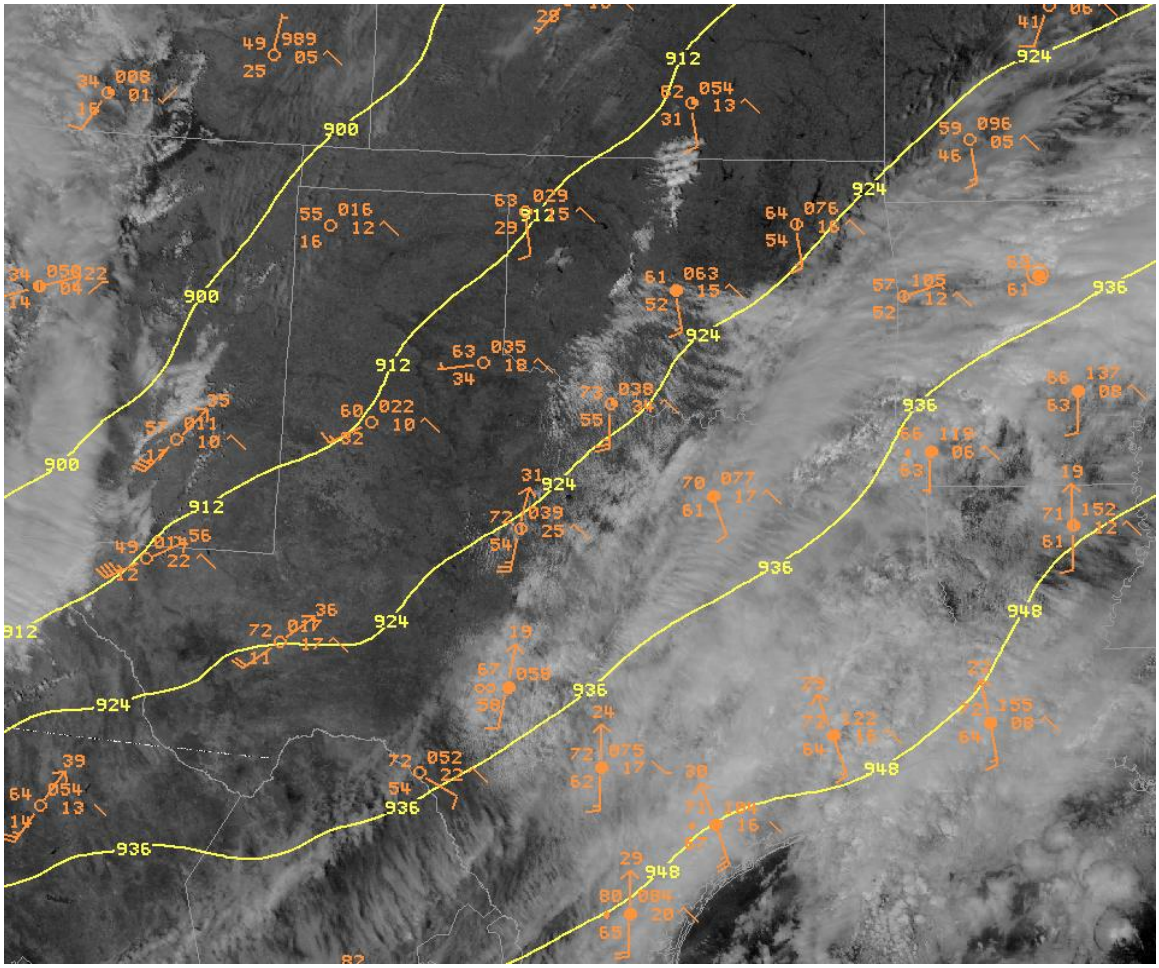

Fig. 2. Composite of surface measurements, 300mb upper air analysis, and *GOES-8* visible image at 1800 10 February 2009. For each station in orange, the temperature (upper left) and dewpoint (lower left) are in °F, and the altimeter setting (right) is in tenths of mb with leading "9 or 10" removed. Full (half) wind barbs represent 5 (2.5) m s^{-1}. Pressure change (middle right) is the change in past 3 hours to nearest tenth of mb. Yellow lines indicate RUC 300mb height analysis in (dam). Cloud features and surface observations provide evidence of the location of the moisture gradient in western OK.

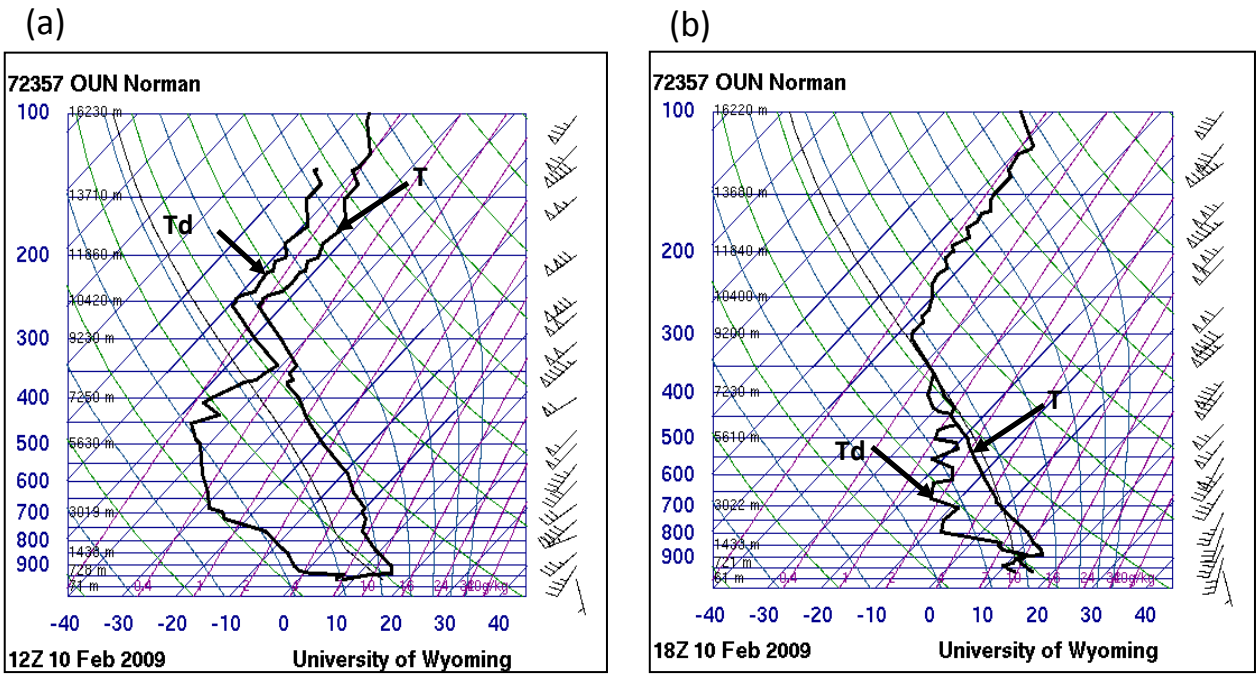

Fig. 3. Environmental conditions near the Oklahoma City supercell. Norman sounding at (a) 1200 UTC and (b) 1800 UTC 10 February 2009. Temperature (T) and dewpoint (Td) are in °C, pressure (left) in mb, and height in m AGL. Wind barbs and flags represent 10 kt (~5 m s^{-1}) and 50 kt (~25 m s^{-1}), respectively.

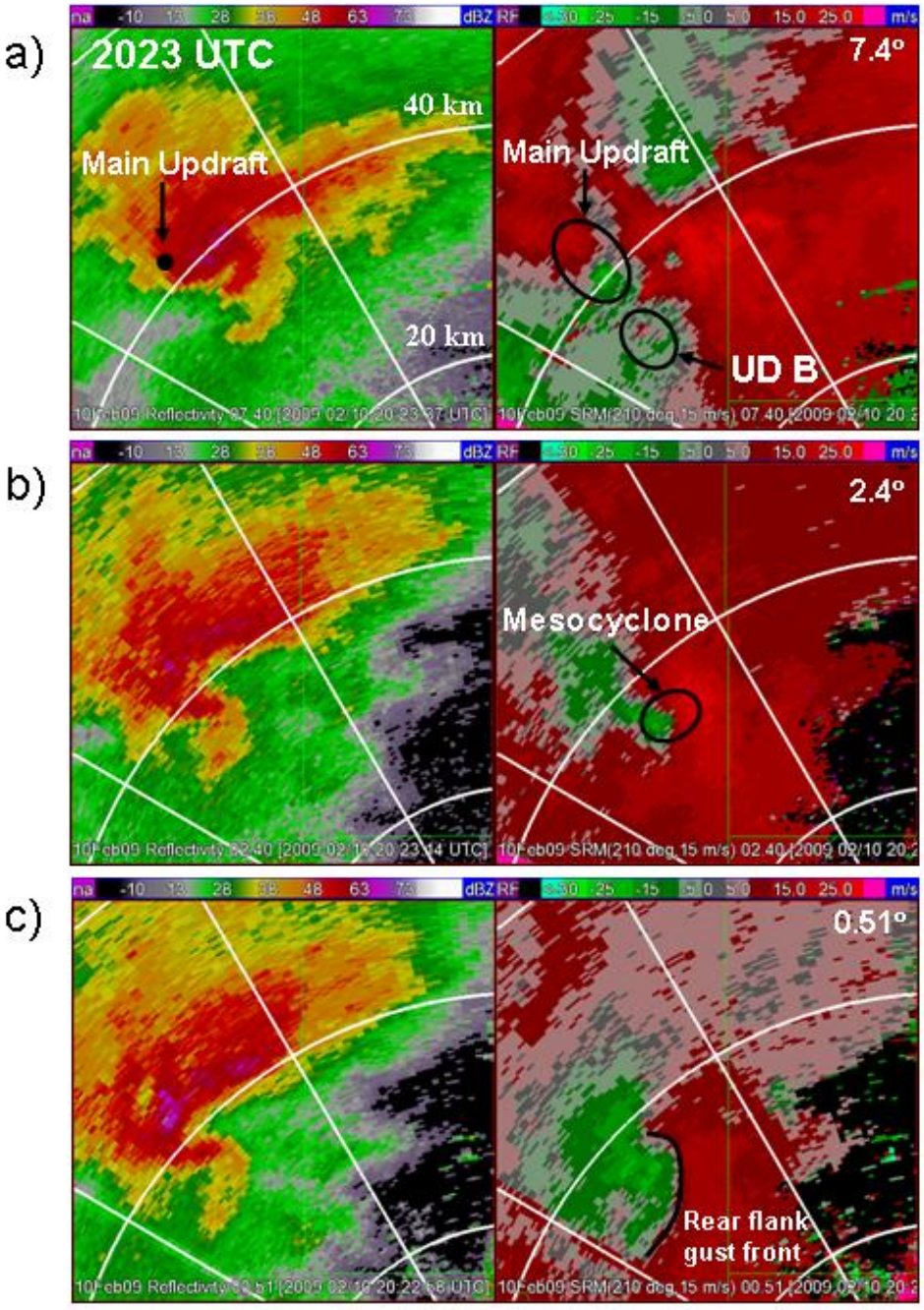

Fig. 4. Reflectivity factor (dBZ) and storm–relative velocity (m s^{-1}) (scales shown on top of each image) at 2023 UTC from the NWRT PAR on 10 February 2009. Range rings (white) are every 20 km. Green lines are county borders: (a) 7.4°, (b) 2.4°, and (c) 0.51°.

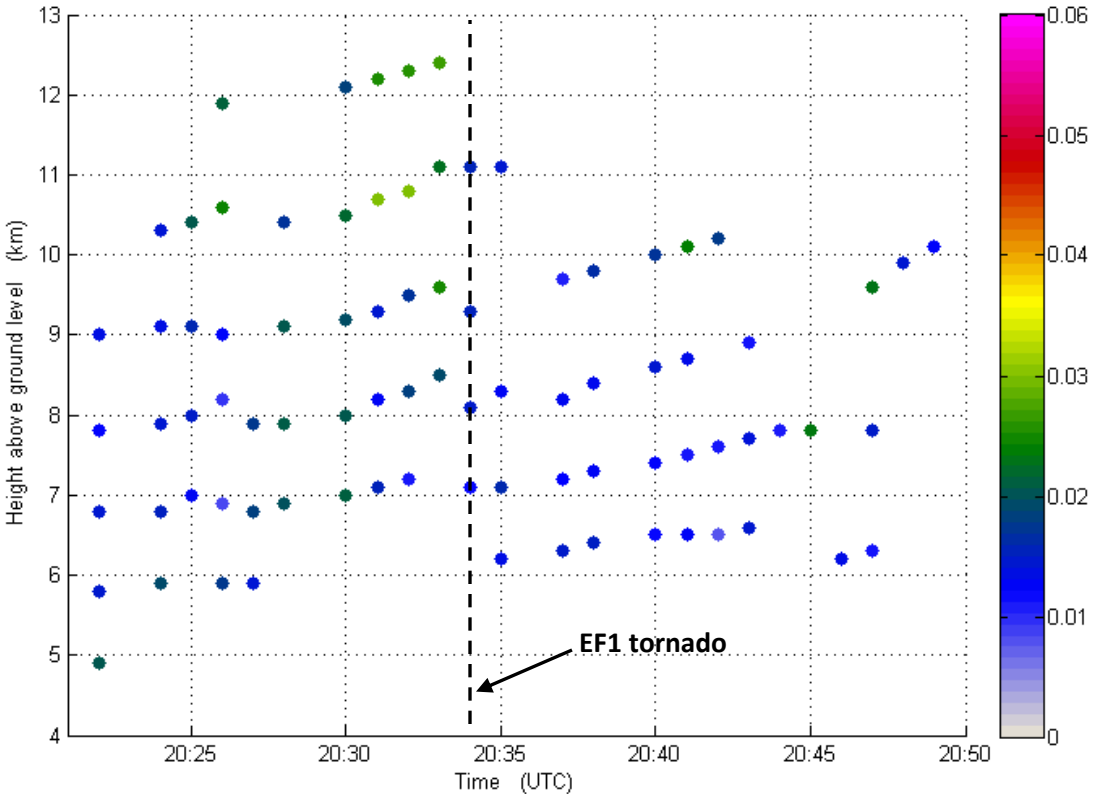

Fig. 5. Time vs. height plot of the maximum divergence of main UD 1. Divergence scale shown on right in s^{-1}.

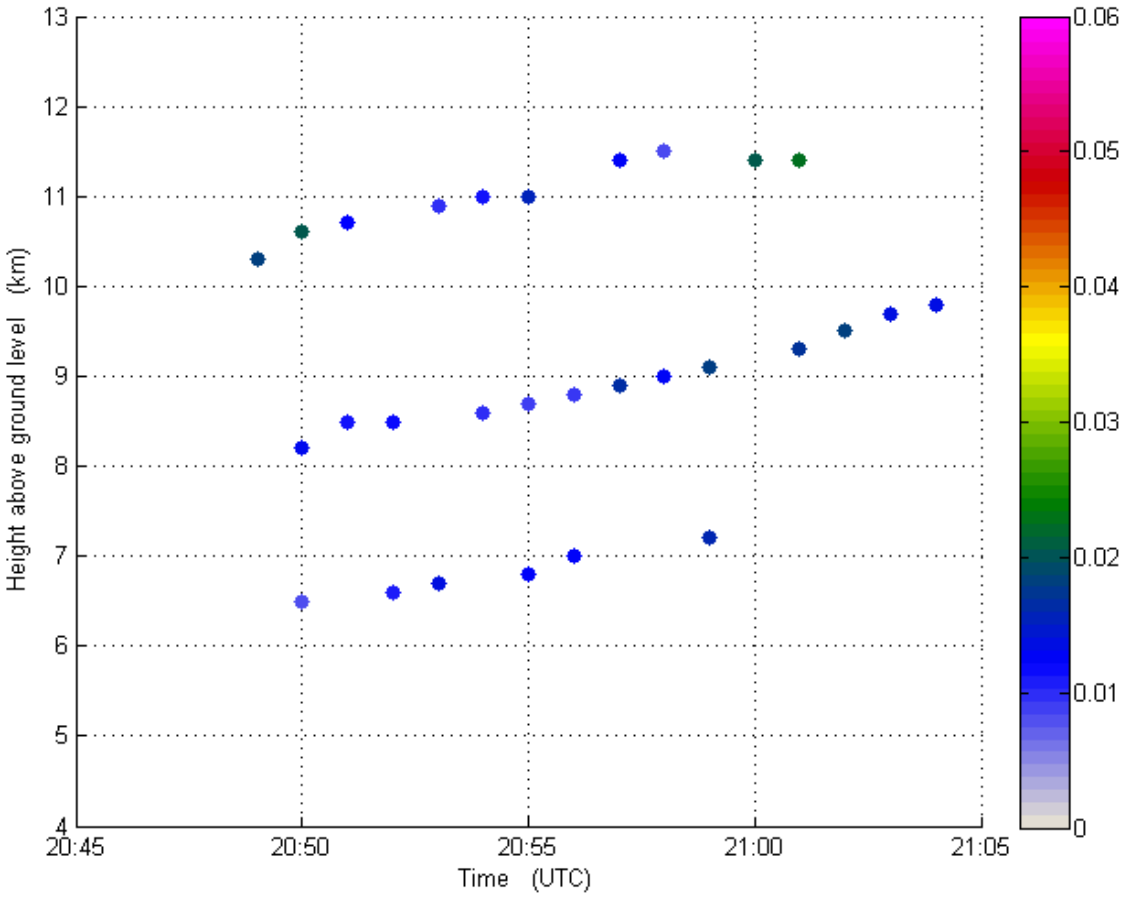

Fig. 6. As in Fig. 4, but: main UD 2.

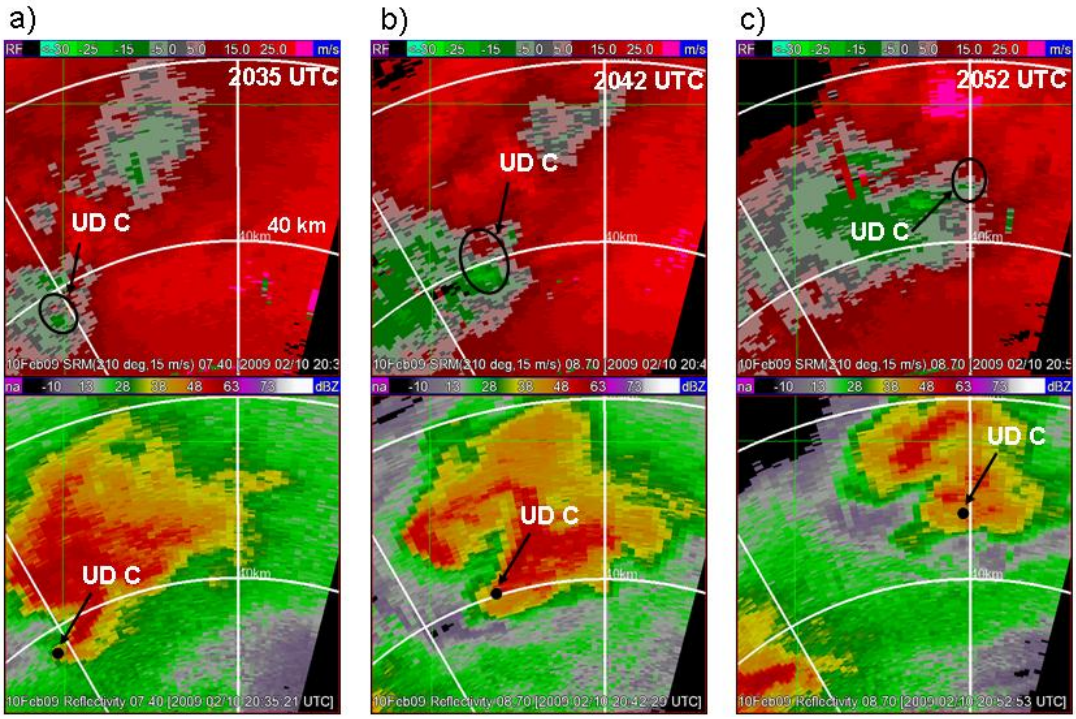

Fig. 7. Reflectivity factor (dBZ) and storm–relative velocity (m s^{-1}) (scales shown on top of each image) from the NWRT PAR on 10 February 2009. Range rings (white) are every 20 km: (a) 2035, (b) 2042, (c) 2052 UTC.

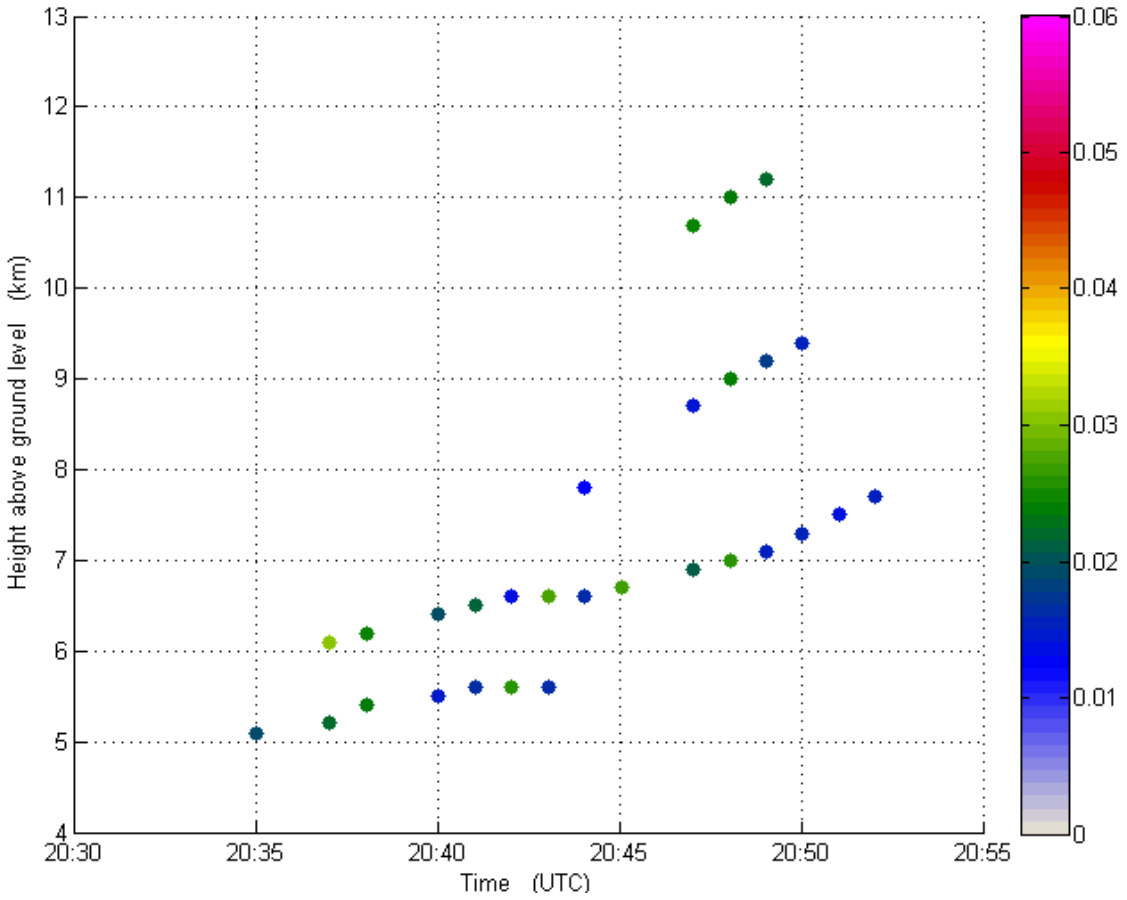

Fig. 8. As in Fig. 4, but: UD C.

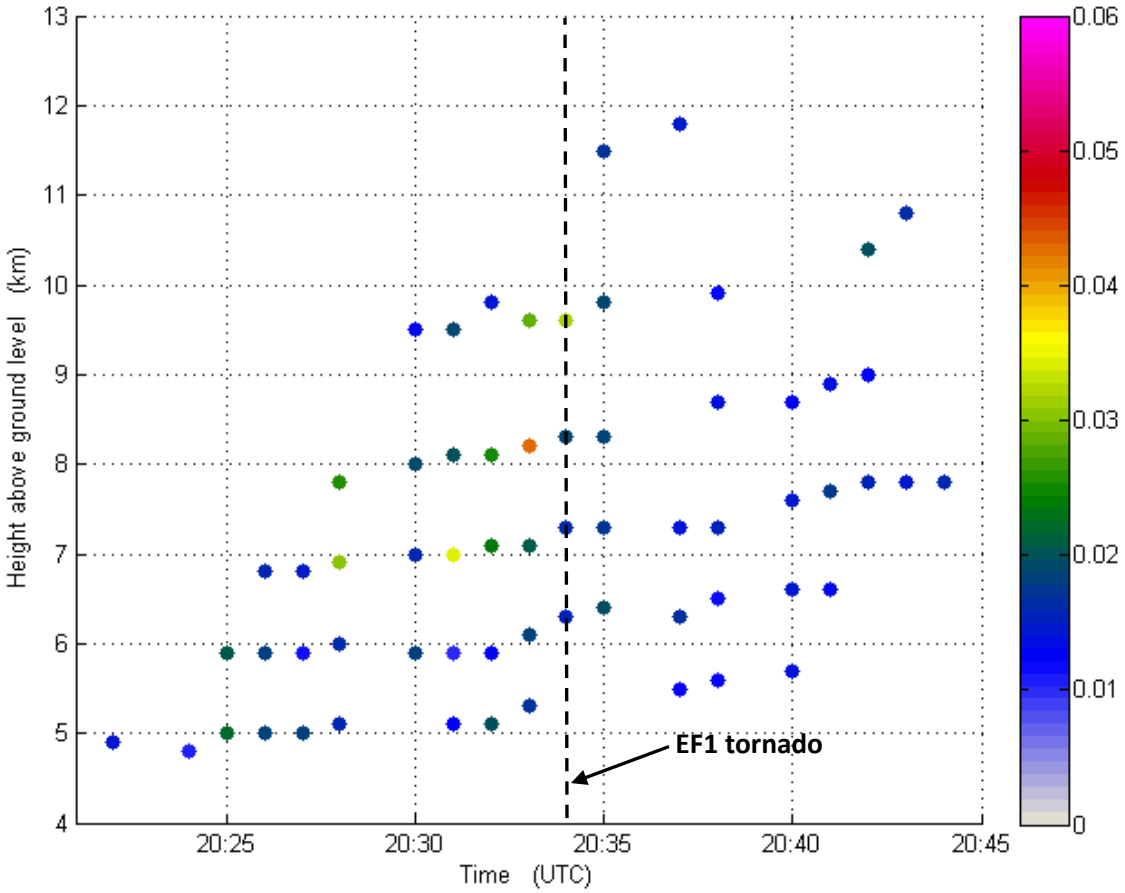

Fig. 9. As in Fig. 4, but: UD B.

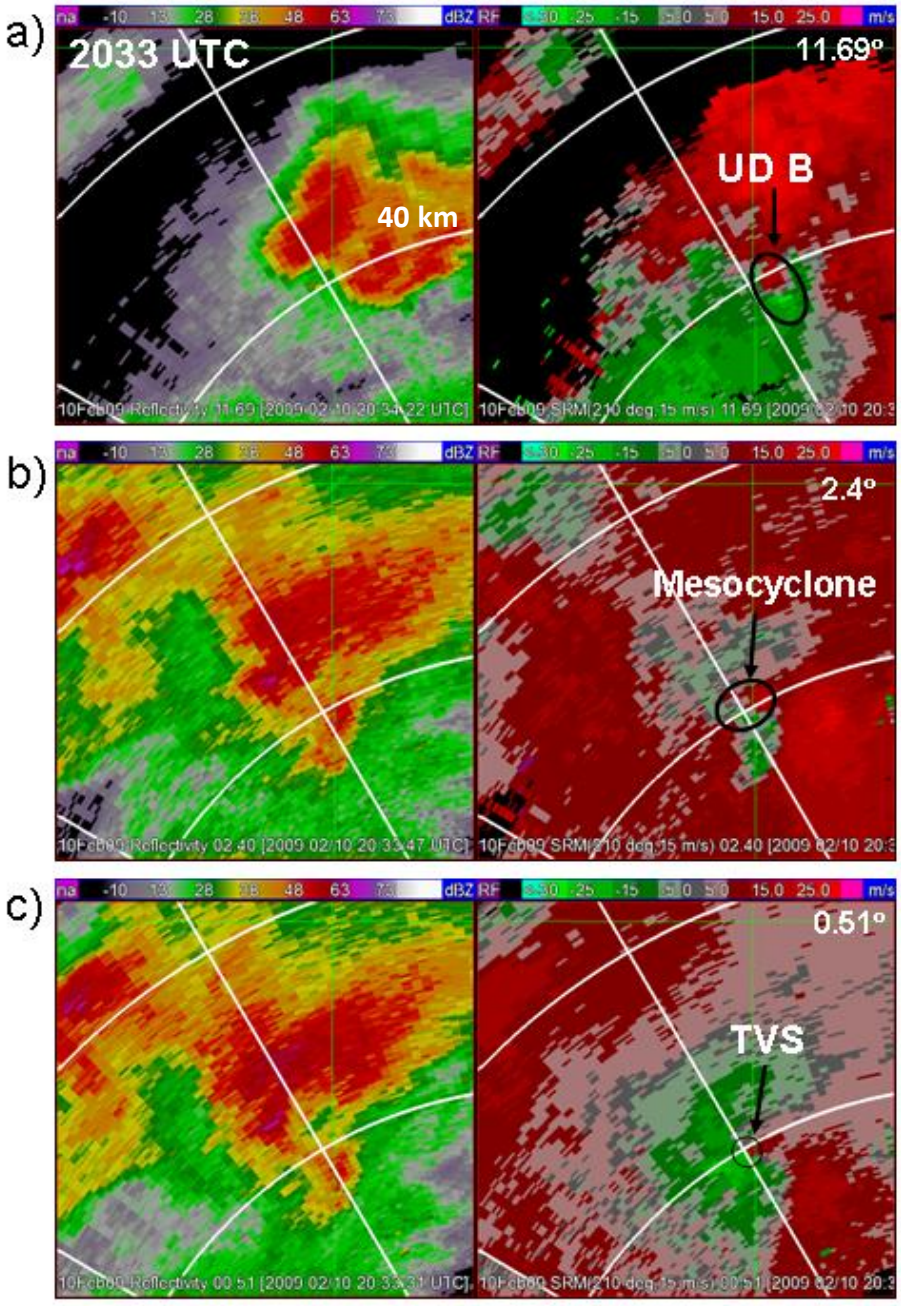

Fig. 10. As in Fig. 4, but: (a) 11.69°, (b) 2.4°, and (c) 0.51°.

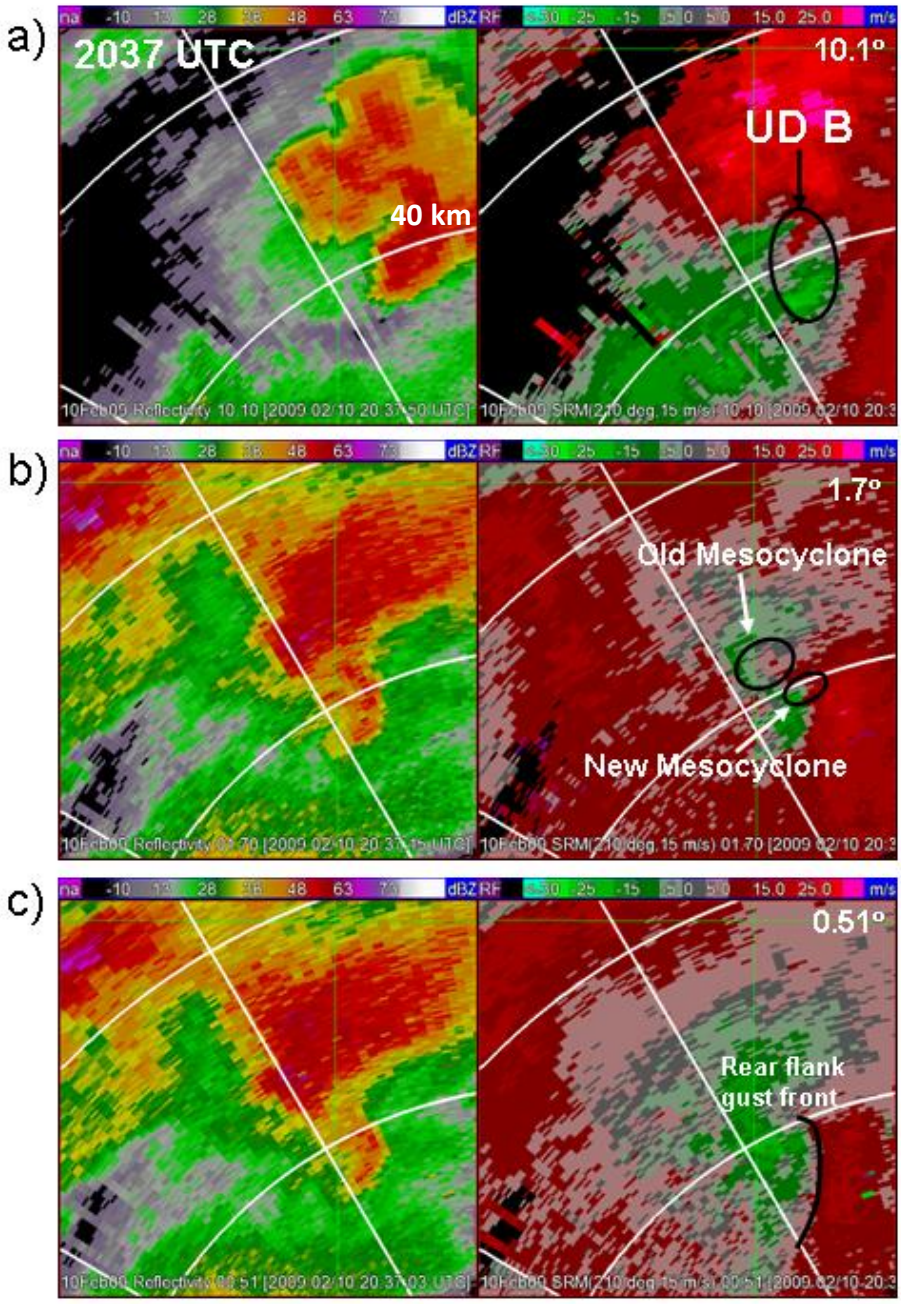

Fig. 11. As in Fig. 4, but: (a) 10.1°, (b) 1.7°, and (c) 0.51°.

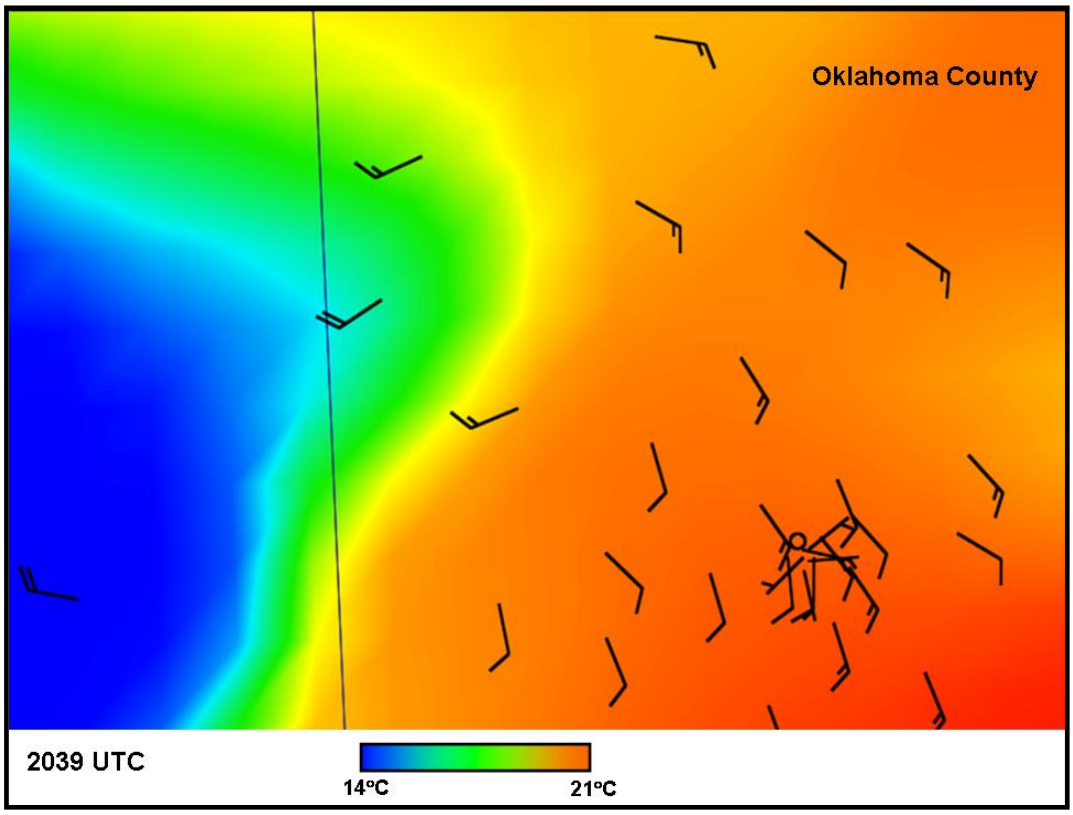

Fig. 12. Composite of Oklahoma City Micronet and Oklahoma Mesonet surface analysis temperature in °C and wind vectors (full barb = 5) m s^{-1} at 10 m AGL. Sharp temperature gradient in western Oklahoma Co. shows gust front with cyclonic circulation at bulge in front.